Int. J. Electrochem. Sci., 10 **(2015)** 1728 - 1741

International Journal of
ELECTROCHEMICAL
SCIENCE
www.electrochemsci.org

Corrosion, Electrical and Mechanical Performance of Copper Matrix Composites Produced by Mechanical Alloying and Consolidation

A. Molina[1], *A. Torres-Islas*[2,*], *S. Serna*[1], *M. Acosta-Flores*[2] *R.A. Rodriguez-Diaz*[1] *and J. Colin*[2]

[1] Centro de Investigación en Ingeniería y Ciencias Aplicadas -UAEM, Av. Universidad 1001, Chamilpa 62209, Cuernavaca Morelos, Mexico.
[2] Facultad de Ciencias Químicas e Ingeniería, Programa Educativo de Ingeniería Mecánica - UAEM, Av. Universidad 1001,Chamilpa 62209, Cuernavaca, Morelos, México.
[*]E-mail: alvaro.torres@uaem.mx

Received: 13 November 2014 / *Accepted:* 19 December 2014 / *Published:* 30 December 2014

FeAl, Fe_3Al and CuNiAl intermetallic particles were added externally to pure copper (Cu) by mechanical alloying and thermal consolidation to obtain intermetallic particles reinforced composites (CuFeAl, $CuFe_3Al$ and Cu(CuNiAl)). The copper metal matrix composites (MMCs) were developed to increase their compressive mechanical resistance without reducing electrical conductivity for spot weld applications related to commercial UNS C1900 copper. Their electrical properties were assessed by electrical conductivity tests, measured in % of IACS (International Annealed Copper Standard), the mechanical properties were obtained by compressive test. Electrochemical impedance spectroscopy (EIS), Potentiodynamic polarization (PP), and Lineal polarization resistance (LPR) techniques, were employed to evaluate the corrosion behavior. The CuFeAl and $CuFe_3Al$ MMCs have the higher corrosion resistance along better electrical and mechanical properties. The electrical and mechanical properties observed are attributed to the presence of the intermetallic particles which induces chemical stability, high lattice order and low density. In the same way, the intermetallic additions induces an structural stability of the passive film preventing the growth of corrosive pittings as the diffusion of metal ions.

Keywords: Copper metal matrix composites; Intermetallic reinforced particles; Mechanical alloying; Electrical and mechanical properties; Corrosion Resistance.

1. INTRODUCTION

Many applications for electronic and manufacturing industry require microstructural stability and high temperature resistance materials in addition to good mechanical properties, high electrical

conductivity and corrosion resistance. For such applications, the most promising metal is copper because of its high electrical and thermal conductivity. However due to its relatively high ductility, is necessary to increase its mechanical resistance being careful not to alter their electrical properties. MMCs have been primarily intended for this purpose. Generally MMCs are composed of two dissimilar materials: a metal matrix, and reinforcing materials in the form of fiber, ceramic, or powder particles [1-3].

The main mechanism of plastic deformation in pure metals and its alloys is the movement of dislocations across the crystal structure [1-3]. In the present work, in order to improve the mechanical strength of pure copper, some powder of intermetallic alloy and a consolidation technique have been developed to introduce obstacles that can prevent the movement and sliding of grain boundaries due to dislocations. The objective is to produce micro or nanometer-sized particles homogeneously dispersed in the copper matrix. These particles must be thermodynamically stable and not overcome by the movement of dislocations. The particle dispersion can be obtained by the mechanical alloying of copper powder and a metal with high tendency to form carbides, oxides or nitrides with the addition of carbon, oxygen or nitrogen, respectively. The resulting agglomerates can be solid solutions or mixtures of phases of micro and/or nanometer size with amorphous or crystalline structures. Several attempts have been done in the last few years to reinforce Copper MMCs to improve the mechanical and electric properties focusing principally on powder metallurgy, casting and amorphous Cu alloys using Ti [1,3,8]. Some other efforts utilize TiB_2, Nb, Al_2O_3, Ti_3AlC_2 and Al-Cu-Fe intermetallic particles [9-15]. Most of the time, MMCs were typically developed to achieve physical and mechanical properties for specific applications, and these were subjected to casual corrosion studies as an afterthought. Conversely, some corrosion and oxidation studies were carried out in Cu MMCs using Fe, TiC, Al and NiCuAl with several compositions [5, 16-20]. On the other hand MMCs find extensive applications in many marine engineering activities because of their light weight, high stiffness and high specific strength [21]. In order to use these materials in marine situations, it is required to withstand corrosive environments, since corrosion decreases the load bearing capacity and thus limit their applications. However, these efforts have been made individually and any attempt is reported yet to integrate mechanical, electrical and corrosion studies to evaluate spot welding copper electrodes and electric connector applications.

In this study, stoichiometric intermetallic FeAl, Fe_3Al and CuNiAl powder particles were used to reinforce pure copper matrix powder (99.7 wt. %) by mechanical alloying. The chemical composition of the intermetallic reinforced powders was varied and the MMCs were characterized by SEM as mechanical and electrical test were carried out to elucidate compressive strength and conductivity. The corrosion behavior of the MMCs in NaCl aqueous solution was also investigated by electrochemical techniques, and compared with those of commercial copper UNS C19000.

2. EXPERIMENTAL PROCEDURE

2.1. Materials and Fabrication

Electrolytic Copper (Cu) powder with purity of 99.7% was used as matrix material. The Cu powder size ranged between 10 and 20 μm. CuNiAl, FeAl and Fe_3Al intermetallic materials were used

as reinforcing agents. Each intermetallic alloy was pulverized by a Pulverisett high energy planetary mill for about 16 h at 400 rpm leading several particulate with different forms and sizes.

Three different MMCs containing up to 5 wt% of CuNiAl, FeAl and Fe_3Al intermetallic reinforcing particles were prepared using mechanical alloying for a period of 12 hours at 600 rpm until a homogeneous mixture is achieved and then placed into containers. The mixed Cu/particles powders were compacted in a tool steel die at 350 °C, using a 60000 Lb hydraulic press. The powders were uniaxial pressed for 2 hours at a compaction pressure of 180MPa. The MMCs produced from the compaction step were subjected to sintering at 600 °C for 1 h. The sintering process was performed under an argon atmosphere. After sintering, the MMCs were subjected to hot extrusion. The MMC billets were extruded at 500 °C. The heating process was carried out using Ni–Cr coils around an upper cylinder. The extrusion reduction ratio was 2:1. The final MMC samples had a cylindrical shape of 5 mm diameter and100 mm length.

2.2. Microstructural, porosity and electrical characterization

Samples extracted from the extruded rods were cut in transverse directions for microstructural and porosity examinations. The bulk porosity of the fabricated MMCs was measured using the water displacement (Archimedean density) approach according to ASTM B962-08 [22]. Cylindrical shape specimens of 5 mm diameter and10 mm length were prepared, grinded and polished by means of silicon carbide abrasive paper under water up to 1200 grit grade. Then, they were polished using first 1 μm alumina powder and then 3 μm diamond paste. Microstructural observations were carried out using SEM and optical microscopy. Electrical conductivity tests were performed using an amperemeter and a Keithley nano-voltmeter. The test consisted on applying a 100mV voltage and registering the current response. The electric resistance was calculated by the Ohm´s law for each MMC. Finally electrical conductivity was obtained as the inverse of their electrical resistance in Siemens (S), $S=1/\Omega$. Alternatively the conductivity can be measured in % of IACS, for temperatures below 20 °C Copper has a electrical conductivity of 100% IACS.

2.3. Micro hardness and Mechanical properties

The MMCs hardness values were measured on polished samples using a Matsuzawa MHT2 microhardness tester. The test was carried out by applying an indentation load of 25g during 15s, with a Vickers indenter according to ASTM B721-91 [23]. A minimum of 15 readings was taken for each sample, and the average value was determined. Mechanical properties were obtained by compressive tests according to ASTM E9-09 [24] in a 10 Tons Universal Machine. Compressive specimens were of the same diameter and length as the MMCs that were microstructural characterized by SEM. Commercial software integrated to the Universal Machine was used for the compressive data recording and acquisition.

2.4. Corrosion tests

The solution volume used in each test was 100 ml prepared with distilled water and analytical grade reagents. Electrochemical tests were carried out in a solution of NaCl (23.5g/L)

Conventional three-electrode arrangement experimental set-up was used for EIS, PP, and LPR tests with a saturated calomel electrode (SCE) as reference electrode and a graphite rod as counter electrode. The electrochemical signals were monitored by AC Gill potentiostat connected to a personal computer. In EIS measurements an alternating current (AC) signal, with an amplitude of 10 mV, was applied at the open-circuit potential (OCP) in the frequency range of 1 MHz to 10 KHz, PP tests were done at 60mV/min sweep rate. The LPR analysis was conducted following the recommendations of the ASTM G 59-91 Standard, polarizing between -100 and +100 mV.

The working electrode area was of 3 mm width, and 8 mm length, masked with acrylic enamel and embedded in poli-acrylic resin with a welded nicromel wire conductor. The samples were grinded up to 600 grit silicon carbide paper, cleaned with water-alcohol and dried under hot air. Immediately the specimens were immersed to the solution in the glass cell.

3. RESULTS AND DISCUSSION

3.1. Microstructure, Mechanical and Electrical Properties

Table 1 shows the chemical composition for each MMC under study and UNS C19000 copper. The morphology for all powders after milling presents a flaky shape with varying sizes between 10 and 50 microns as shown in Figure 1a for the CuFeAl composite. Figure 1b presents mechanical consolidated powders for the Cu (CuNiAl) composite it can be observed that consist of a pileup of powder layers that are compacted one over each other. There is not diffusion between them, showing clearly the gaps among particles. Such characteristic was present in all the mechanical consolidated powders under study. Once the mechanical powders were sintered the SEM analysis showed that all of the MMCs have equiaxed grains with the presence of twins, observed as straight lines within the grains, see figures 2a, 2b and 2c. It has been reported [1] that such type of lattice defects are developed by a severe deformation during milling, leading to the formation of crystalline and quasi-crystalline ductile phases in this type of materials. This could promote the formation and propagation of shear bands affecting the MMCs ductility and toughness [1]. Most of these defects have been observed at nano-scales, however in this study we can see it at micron levels as illustrated by Figures 2a, 2b, and 2c. The observed twins within the MMCs grains can be the result of accumulation of nanosized shear bands. As showed in Table 2 CuFeAl, $CuFe_3Al$ and Cu(CuNiAl) has major toughness with respect to Copper UNS C19000, so an explanation of their higher toughness could be described as due to the atomic glide opposition of the twins, eventually increasing the mechanical resistance. From the same table it was evident that the Cu(CuNiAl) presents the highest Young's Module (E), followed in decreasing order, by the CuFeAl,$CuFe_3Al$ and at last the UNS C19000 copper. In this way, we can say that the number and amount of alloying elements can contribute to enhance their mechanical properties

at atomic level (Young's Modulus) as it can be seen in figure 3 that shows the stress-strain behavior of CuFeAl, $CuFe_3Al$ and Cu UNS.

.

Table 1. Composite and Copper UNS 19000 composition

		Reinforcement (wt %)				
Composite	Cu (Matrix wt%)	Cu	Fe	Al	Ni	P
Cu(CuNiAl)	95	1.5		1	2.5	
CuFeAl	95		3.5	1.5		
$CuFe_3Al$	95		4	1		
Cu UNS 19000	98.7				1.1	0.25

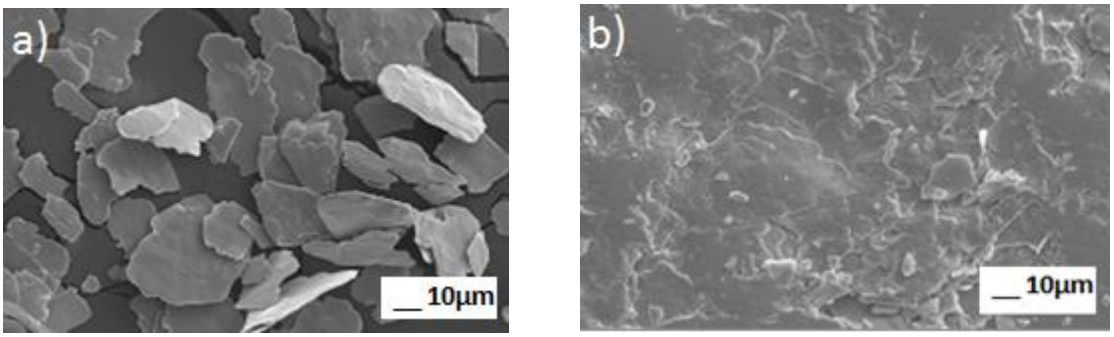

Figure 1. (a) SEM micrograph of powders after milling of CuFeAl reinforced composite and (b) consolidated composites

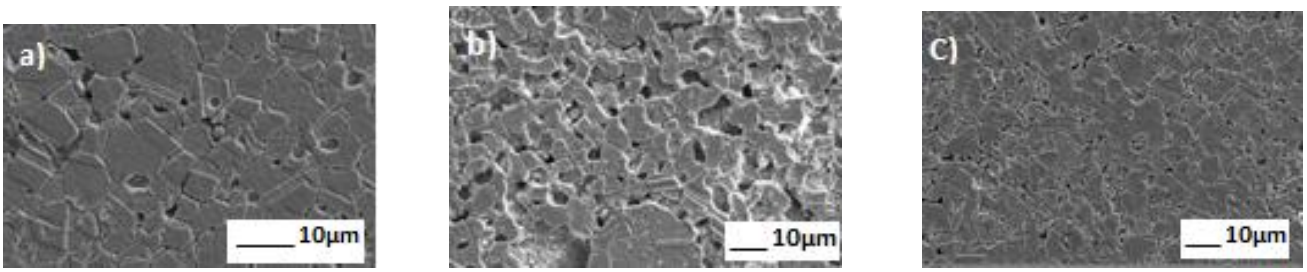

Figure 2. (a) SEM micrograph of sintered CuFeAl composites (b) Cu(CuNiAl) composites and (c) $CuFe_3Al$ composites

Table 2. Composite and Copper UNS 19000 density, hardness, mechanical and electric properties

	Density (gr/cm^3)	Hardness (HV)	E (Gpa)	σy (MPa)	Deformation (%)	R (Ω)	IACS (%)
CuFeAl	6.7	71.68	3.81	210 .34	7.76	6.89E-06	85.49
Cu (CuNiAl)	6.47	71.34	4.13	187.85	5.75	6.82E-06	85.4
$CuFe_3Al$	5.89	57.29	3.79	175.38	5.49	1.03E-05	57.94
Cu UNS	8.9	40	1.4	100.2	5.15	1.01E-05	55

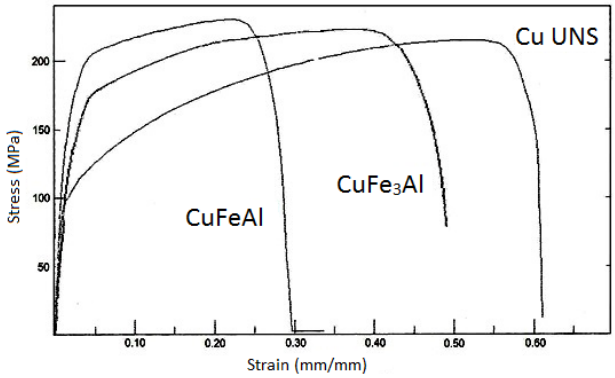

Figure 3. Stress-strain behavior of CuFeAl, $CuFe_3Al$ and Cu UNS.

On the other hand the CuFeAl present the peak Vickers and IACS values among all other materials tested in the present work. Although, Cu(CuNiAl) has a minor conductivity value than CuFeAl present the major Young Modulus (E) pointing this composite as the best balanced MMCs within their mechanical properties and electrical conductivity. Recently, Brosseau[2] while modeling the electromagnetic waves with nanocomposites has reported that each phase present in composite materials has particularly properties related to their atomic array and microstructure. This generates clusters that act as small systems that collectively interact with other similar phases thus magnifying their original properties such as the mechanical and electrical properties. However this behavior has been reported on a nanoscale level on composites, the evidence presented in Table 2 related to mechanical and electrical properties suggests that the principles reported by Brosseau[2] could be applied to the MMCs systems under study.

Regarding the MMCs hardness values, the authors found a correlation as stated by Chang Kyu et al [3] with respect to their densities and chemical composition. Chang Kyu et al described that an increase in the copper quantity leads to a decrease in the hardness values of MMCs and as table 2 shows, our actual MMCs hardness values trend to be diminished as the copper content increase which agrees with that reported from Chang elsewhere [3]. In this way the material with the lowest hardness value was for the UNS C19000 Copper. Similarly, it was appreciated from Table 2 that at major density values in the Cu composites and upgrade in their corresponding Vickers hardness numbers take place too. The MMC CuFeAl exhibits the minor porosity level as seen in Figure 2. The porosity has a relevant roll in the mechanical properties and electrical conductivity, this could be explained in terms of the contact surface between the material grains. Indeed the electrical conductivity would be major in the CuFeAl as well as their mechanical properties because more grains are in contact.

3.2. Corrosion tests

3.2.1 Potentiodynamic polarization curve and LPR Measurements

Figure 4 shows the potentiodynamic polarization curves of the MMCs and copper UNS C19000 respectively immersed in stagnant 3% wt NaCl solution. The fitted values of corresponding

kinetic parameters such as corrosion potential (E_{corr}), corrosion current density (I_{corr}), anodic and cathodic Tafel slope (b_a,b_c) and corrosion rate (Corr rate) are listed in Table 3. The corrosion potentials to Cu UNS C19000 and Cu (CuNiAl) are more positive than CuFeAl and $CuFe_3Al$. Furthermore, both the anodic and cathodic Tafel slopes of the polarization curves of CuFeAl and $CuFe_3Al$ are larger than Cu UNS C19000 and Cu (CuNiAl), which indicates that both the anodic and cathodic processes are to some extent inhibited due to the formation of more protective corrosion product film to CuFeAl and $CuFe_3Al$ MMCs. In addition corrosion current densities (i_{corr}) were determined by Tafel extrapolation method from Figure 4 and correlated to a corrosion rate value in mm/year (see Table 3), based on Faraday's law. [25] The CuFeAl, and $CuFe_3Al$ had smaller i_{corr} values and corrosion rates in mm/year than copper UNS C19000 and the Cu(CuNiAl) composite. The latter exhibits the worst corrosion resistance compared to copper UNS C19000 and as noticed by their i_{corr} values, the addition of the CuNiAl intermetallic to pure copper has the harmful effect for the NaCl solution corrosion resistance.

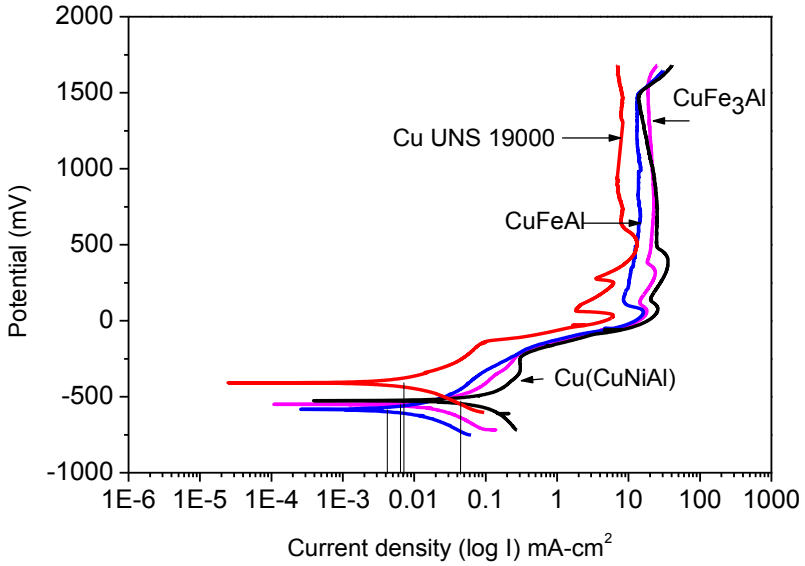

Figure 4. Polarization curves of composites and copper UNS 19000 in NaCl solution

Table 3. Corrosion parameters of composites and copper UNS 19000 in NaCl solution by potentiodynamic polarization

Material	E_{corr}	I_{corr}	Corr rate	ba	bc
	(mV_{SCE})	(mA-cm²)	(mm/year)	(mV/decade)	(mV/decade)
CuFeAl	-586	0.0042	1.12	161	-245
$CuFe_3Al$	-540	0.00633	1.73	149	-268
Cu UNS C19000	-406	0.00714	1.8	75	-100
Cu (CuNiAl)	-526	0.04465	8.46	72	-104

According to Figure 4 and Table 3, all of the specimens exhibited active corrosion and passivation behavior near a potential of +49 mV_{SCE}. Also, Table 3 shows that if the corrosion potential (E_{corr}) get lower values; correspondingly the I_{corr} presents decreasing values for all materials tested. Commonly, any alloy or material can slow their corrosion rates by its ability to generate a stable protective surface layer that is made of corrosion products that leads to the protection of the material itself. In these terms, copper UNS C19000 would better suppress corrosion rate while a superficial protective layer is present. It present the major passivity level, their passivity region was extended beyond the +1700 mV_{SCE}, while, the CuFeAl and Cu(CuNiAl) pitting potentials were present at +1490 mV_{SCE}. The $CuFe_3Al$ presents a higher pitting potential (+1590 mV_{SCE}) showing better corrosion protection again among all MMCs.

Figure 5 show the LPR test results, polarization resistant (Rp) varies over time for the copper UNS C19000 and all MMCs studied under the NaCl solution. For the CuFeAl and $CuFe_3Al$, Rp increases with time, indicating a decrease in the corrosion rate with elapsed time after approximately 7 hours immersion in NaCl solution. These composites present their upper Rp values on 58 Ω-cm^2 and 70 Ω-cm^2 respectively. Their initial Rp values are low but then became higher with almost a steady growing suggests the formation of a durable protective film. UNSC 19000 copper present the most elevated Rp values (90Ω-cm^2) but their behavior over time is completely irregular. This behavior represents a material that can be protected but at the same time their protective corrosion layer was prone to be destroyed. However, copper can regenerate the corrosive film easily thus presenting the random performance. At last the Cu(CuNiAl) present the worst behavior and the lowest Rp values (17 Ω-cm^2 after 7 hours) contrary to the other two composites. The Cu(CuNiAl) could develop a surface film, but is a non-adherent layer which can be easily removed from the composite surface and cannot protect it under the environmental conditions used here. As shown by the Polarization Curves (Figure 4), the LPR results also suggest that the film protectiveness should depend on their adherence and stability and to the superficial conditions of each material related to the corrosion environment.

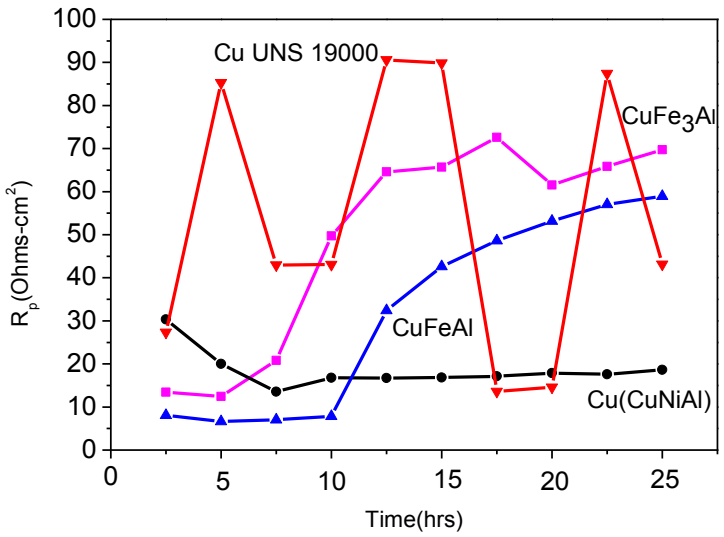

Figure 5. LPR behavior of composites and copper UNS 19000 in NaCl solution

To explain the corrosion behavior presented by the CuFeAl and $CuFe_3Al$ that were the more favorable MMCs to withstand corrosion, elements such as Cu, Fe, and Al that are important alloys in these composites were evaluated in the Pourbaix diagrams [4]. This was done under the neutral pH 7 conditions and E_{corr} values as showed by their corresponding polarization curves (Table 3). The results reveal that Cu is immune but the Fe corrodes forming Fe_3O_4 and FeO. However, aluminum gets passivated forming a protective layer of Trihydrated aluminium oxide (Al_2O_3-$3H_2O$) also known as hydrargillite, this layer is sufficiently compact to reduce composite dissolution. The Fe corrosion products (Fe_3O_4 and FeO) are not soluble in the corrosion solution but can be mixed or agglutinated to the hydrargilite forming a more protective film over the surface composites. Binczyk et al [5] present evidence of the after mentioned mechanisms studying the AlCuFeCr system under XRD and EDS techniques that were in contact to neutral aqueous corrosion solutions. For this investigation the passive performance illustrated by the LPR and Polarization curves in these particularly composites could confirm that these mechanism are present too under the NaCl corrosion solution used.

Related to pure copper and its alloys they are unique among the corrosion-resistant alloys in that they do not form a truly passive corrosion product film. In aqueous environments at ambient temperatures, the corrosion product predominantly responsible for protection is cuprous oxide (Cu_2O). This Cu_2O film is adherent and follows parabolic growth kinetics. [6] Cuprous oxide is a *p*-type semiconductor formed by the following electrochemical processes:

$$4Cu + 2H_2O \rightarrow 2Cu_2O + 4H^+ + 4e^- \text{ (anode)} \qquad \text{(Eq 1)}$$

and

$$O_2 + 2H_2O + 4e^- \rightarrow 4(OH)^- \text{ (cathode)} \qquad \text{(Eq 2)}$$

with the net reaction: $4Cu + O_2 \rightarrow 2Cu_2O$.

For the corrosion reaction to proceed, copper ions and electrons must migrate through the Cu_2O film. Consequently, reducing the ionic or electronic conductivity of the film by doping with divalent or trivalent cations should improve corrosion resistance. In practice, alloying additions of aluminum, zinc, tin, iron, and nickel are used to dope the corrosion product films, and they generally reduce corrosion rates significantly. For the present investigation copper UNS C19000 present relatively good corrosion rates although their corrosion resistance values were below the CuFeAl and $CuFe_3Al$ composites. However copper UNS C19000 presents and unusual behavior showed by their LPR values related to continuous dissolution and passivation. This suggests that copper effectively suppress its superficial corrosion but only when the protective Cu_2O layer is stable. Over time evidence (Figure 5) shows that this protective layer can be destroyed but quickly regenerated. This protective layer performance could be related to that this superficial layer is not a truly passive corrosion product film. But, as showed by Table 2 nickel act as a dopant to Cu that helps to reduce its corrosion rate, as mentioned earlier.

Conversely In NaCl solution pH≈7 galvanic corrosion of galvanic couple composed of Cu(CuNiAl) would occur on the surface of composite because nickel, copper and aluminum powder have different electrode potential (φNi—0.136 V, φCu+0.337 V, φAl—1.66 V) [7]. Among these galvanic couple, nickel and aluminum powder due to their lower electrode potential would be the top priority to being oxidized to Ni^{2+} and Al^{3+} ions that would diffuse into bulk solution. Although aluminum powder of CuNiAl galvanic couples are easily oxidized, the corrosion process of aluminum powder would be stopped or slowed because of compact oxidation film produced from the galvanic corrosion covering on aluminum powder surface. And the copper and nickel powder would also be corroded in water. Hence, in the NaCl solution, galvanic corrosion reactions occurring on the surface of composite are as follows: Anode: $Cu \rightarrow Cu^{2+}+2e$; $Ni \rightarrow Ni^{2+}+2e$; $Al \rightarrow Al^{3+}+3e$ Cathode: $O_2+H_2O+4e \rightarrow 4OH^-$ These galvanic corrosion reactions cause Cu^{2+}, Ni^{2+}, and Al^{3+} ions cumulate in the surface of composite. Besides, being driven by the ion concentration gradient, there would be an amount of $Ni^{2+,}$ Cu^{2+} and Al^{3+} ions in bulk solution. Those metal ions intensively inhibit the nucleation and growth rate of hydrargillite on the surface of composite increasing dissolution rates.

3.2.2 Electrochemical impedance spectroscopy studies

The measured impedance spectra of the CuFeAl, $CuFe_3Al$, Cu(CuNiAl) composites and copper UNS C19000 in the NaCl solution are shown as Nyquist plots in Fig. 6, and Bode diagrams in Figs. 7 and 8, respectively. It is evident from Fig. 6 that all materials exhibit a tendency to form a semicircle indicating a charge transfer corrosion mechanism.

CuFeAl and $CuFe_3Al$ MMCs present the higher Z'' values as shown in their corresponding Nyquist diagrams on Figure 6. This indicates an elevated capacitance (C_{dl}) value in the metal solution interphase with the presence of a high charge transfer gradient that could be related with the formation and permanence of a passive layer. For each one of these composites the Nyquist semi-circles have started at $Z'=0$, thus the solution resistance (R_s) was practically zero and the Na^+ and Cl^- ions present in the NaCl electrolyte were always free to move in the aqueous environment. This behavior coincides with the polarization results that show that the oxide generated do not diffuse to the solution and just interact with the composites surface to form the passive layer. As a result and evidenced by Figure 7 their impedance modulus |Z| are greater with respect to copper UNS C19000 and the Cu(CuNiAl) composite.

For the Cu(CuNiAl) Nyquist diagram (Fig 6) it is observed at high frequencies that the data points tend to form a straight line at 45° with respect to the Z' axis. Generally this was related to a diffusion corrosion mechanism although going further to lower frequencies in the same plot the tendency was to form a semi-circle. Also, from the same graph was noticeable that the Cu(CuNiAl) Nyquist curve begins approximately at 15 Ohm-cm^2. This indicates that the migration of the byproducts corrosion ions: Ni^{2+}, Cu^{2+} and Al^{3+} to the solution was possible, thus diminishing its Z'' and |Z| values as shown in Figures 6 and 7 respectively. So, all these evidence (Figures 4, to 7) point out that Cu(CuNiAl) forms a weak and permeable layer that can be dissolved over time allowing the continuous corrosion of the composite.

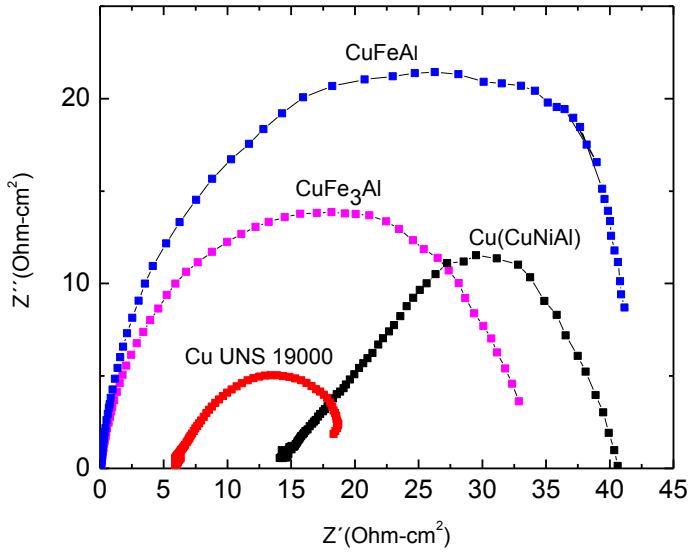

Figure 6. Nyquist plot for composites and in NaCl solution

The Nyquist curve for pure copper on Figure 6 shows that the principal corrosion mechanism was charge transfer. Pure copper also present and offset of the beginning of their graph increasing its R_s value and also a low C_{dl} value (5 Ohm-cm^2) and the lowest |Z| value among all materials tested. This copper UNS19000 impedance corrosion behavior is in accordance to that already stated by their corresponding LPR and polarization curves, about copper corrosion mechanism and corrosion resistance. That is in order to corrosion reaction proceed, copper ions and electrons must migrate through the Cu_2O film to solution showing and increase in their R_s value, and do not form a truly passive corrosion product film.

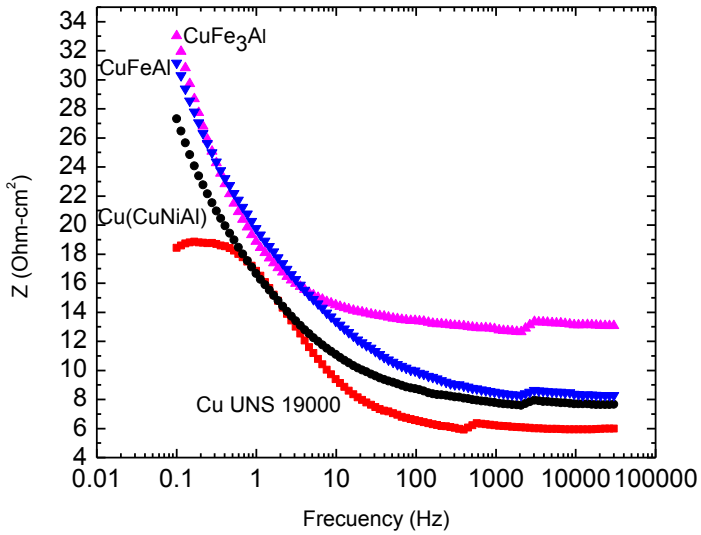

Figure 7. Bode impedance plot for composites and copper UNS19000 in NaCl solution

In order to have a better insight on the passivity response as well as the charge transfer and diffusion phenomenon, Bode phase angle plots (Fig. 8) were constructed. As already seen, the CuFeAl, and $CuFe_3Al$ composites offer relatively better corrosion resistance than Cu(CuNiAl) composite and copper UNS C19000 that leads to an increase in their corrosion protective ability. The Bode phase angle plots of the CuFeAl, and $CuFe_3Al$ composites suggested the involvement of one time constant characteristic of active corrosion and thus it is concluded that only one mechanism prevailed for the corrosion composites. In accordance with Binczyk [5] this occurrence could be related to the electrolyte/composite interface. Almost active corrosion behavior in both composites, lead a trend in Bode angle plots to continue in a relative constant degree value, which indicates the continuous presence of a passive film on composite surface. In contrast Cu(CuNiAl) composite and copper UNS C19000 in their corresponding Bode angle plots (Fig. 8) shows a steady phase angle decrease at low frequency. This confirms the presence of a passive film that decreases their protective properties with respect to time and frequency**.**

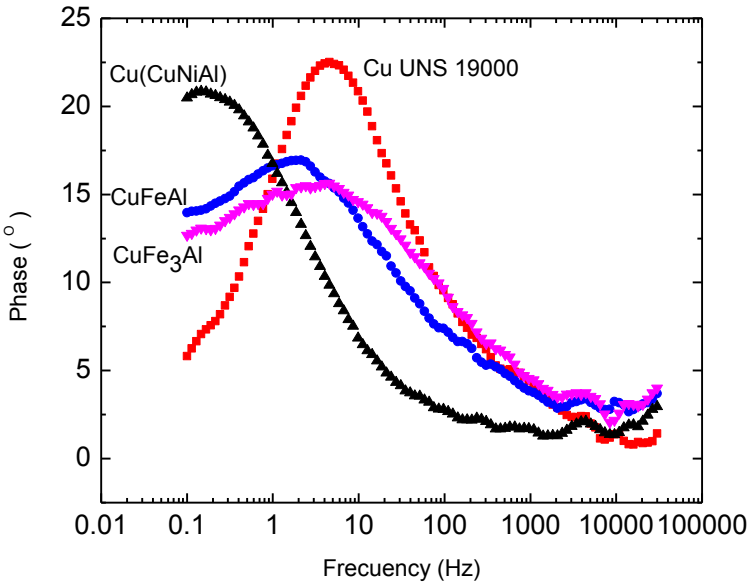

Figure 8. Bode Phase plot for composites and copper UNS19000 in NaCl solution

4. CONCLUSIONS

Mechanical alloying and sintering are good manufacturing routs for the fabrication of metal matrix composite materials in this case pure copper UNS C19000 was reinforced with FeAl, Fe_3Al and CuNiAl intermetallic powders. Under mechanical point of view the FeAl, CuNiAl, and Fe_3Al powders reinforce very well pure copper, however Fe_3Al impairs minor ductility to the MMC so the FeAl are more suitable for compressive stress applications. Their hardeness values are more or less similar in that FeAl (71.68 HV) present the greatest value followed by the CuNiAl, Fe_3Al, and at last pure

copper. Their mechanical behavior can be explained due to the atomic glide opposition of their twins as showed in their microstructures, eventually increasing their mechanical resistance of the MMC. Corresponding to their conductivity values in IACs here the MMC reinforced with the FeAl particles showed the best value. The porosity has a relevant roll in the mechanical properties and electrical conductivity, this could be explained in terms of the contact surface between the material grains. Indeed the electrical conductivity would be major in the CuFeAl as well their mechanical properties because more grains are in contact

From the corrosion point of view the CuNiAl particles contrary to the behavior showed by the other two intemetallic powders (FeAl and Fe_3Al) lower the MMC corrosion resistant, even present lower corrosion properties than pure copper.

The CuFeAl and $CuFe_3Al$ achieved their good composite properties and corrosion performance principally due to: reinforcing particle chemical stability, density, lattice arrangement, effective metallic area prone to corrosion, structural state of the passive film, ability to prevent diffusion of metal ions, porosity or defect size of the sintered composite, and the ability of the particle to prevent the corrosive pits from growing up. Leading them to be very promising new advanced engineering materials that can substitute the commercial copper UNS C19000 electrodes under the requirements for spot welding and possibly for marine industry applications.

References

1. R.H.Palma, H.Sepulveda, A. Aquiles, R.Espinoza, R.C.Montiglio, *J. Mater. Process Tech*, 169 (2005) 62
2. C.Brosseau, J. Nanomater, (2007) Modeling and Characterization of the Interaction of Electromagnetic Wave with Nanocomposites and Nanostructured Materials, Article Id 74545 1-2
3. K.K.Chang, S. Lee, S.Y.Shin, D.H.Kim, *Mat.Sci.Eng A*, 449-451 (2007)
4. M.Pourbaix, Atlas of Electrochemical Equilibrium in Aqueous Solutions NACE , Houston Texas, (1974)
5. E.Binczyk, N.Homazava, A.Uldrich, R. Hauert, M.Lewandowska, , K.J. Kurzydlowski, P.Schmultz, *Corros.Sci*, 53 (2011) 1825
6. ASM handbook vol. 13, Corrosion, Materials Park, ASM International, OH, (2001)
7. G.Song, B.Johannesson, S.Hapugoda, D. St. John, *Corros.Sci*, 46 (2004) 955
8. M.Kikuchi, Y.Takada, S.Kiyosue, M.Yoda, M.Woldu, Z. Cai, O.Okuno, T. Okabe, *Dent Mater*, 19 (2003) 174
9. M.Lopez, D.Corredor, C.Camurri, V.Vergara, J.Jimenez, *Mater. Charact*, 55 (2005) 252
10. C.L. Quin, W. Zhang, K. Kimura, X.M. Wang, A. Inoue, *Acta Mater*, 54 (2006) 3713
11. E.Botcharova, J.Freudenberger, L.Schultz, *Acta Mater*, 54 (2006) 3333
12. R.Viseslava, D.Bozic, M.T.Jovanovic, *J.Alloy. Compd*, 459 (2008)177
13. L.Peng, *Scripta Mater*, 56 (2007) 729
14. H.C.Lin, Y.Du, H,Xu, W.Xiong, *J.Mater.Res*, 24,10, (2009) 3154
15. G.Laplanche, A.Joulain, J.Bonneville, R.Schaller, T.El Kabir, *J.Alloy Compd*, 493 (2010) 453
16. T.Liu, H.Shao, X.Li, *Nanotechnology* 14 (2003) 545
17. P.Molera, S.F.Sanz, J.J.Suñol, *Mater.Corros*, 57 (2006) 568
18. J.Zhu, L.H.Hihara, *Corros.Sci*, 52 (2010) 406
19. S.Faraji, A.R.Abdul, N.Mohamed, S.Stephen, B.R.Coswal., *Arab.J.Chem*, 6 (2013) 379
20. G.G.Wang, L.Q.Zhu, H.C.Liu, W.P. Li, *Surf. Coat. Tech*, 206 (2012) 3728

21. ASM handbook vol. 21. Composites, Materials Park, ASM International, OH, (2001)
22. Standard test methods for density of compacted or sintered powder metallurgy (PM) products using Archimedes principle, ASTM B962-08, American Society for Testing and Materials, Philadelphia, PA, USA, (2008)
23. Standard test method for microhardness and case depth of powder metallurgy (P/M) parts, ASTM B721-9. American Society for Testing and Materials, Philadelphia, PA, USA, (1999)
24. Standard test methods of compression testing of metallic materials at room temperature ASTM E9-09. American Society for Testing and Materials, Philadelphia, PA, USA, (2009)
25. D.A.Jones, Principles and Prevention of Corrosion, 2nd ed., Prentice-Hall, USA, (1996)